**This is the Pre-Published Version.**

The following publication J. Zhou et al., "Digital Signal Processing for Faster-than-Nyquist Non-Orthogonal Systems: An Overview," 2019 26th International Conference on Telecommunications (ICT), Hanoi, Vietnam, 2019, pp. 295-299 is available at https://doi.org/10.1109/ICT.2019.8798855.

# Digital Signal Processing for Faster-than-Nyquist Non-Orthogonal Systems: An Overview

Ji Zhou[1,*], Mengqi Guo[2], Yaojun Qiao[2,†], Haide Wang[1], Long Liu[1], Weiping Liu[1], Changyuan Yu[3], Jianping Li[4] and Zhaohui Li[5,‡]

[1]Department of Electronic Engineering, Jinan University, Guangzhou, China

[2] School of Inform. and Commun. Engineering, Beijing University of Posts and Telecommunications, Beijing, China

[3]Dept. of Electron. and Inform. Engineering, Hong Kong Polytechnic University, Hongkong, China

[4]Institute of Photonics Technology, Jinan University, Guangzhou, China

[5]State Key Lab. of Optoelectronic Materials and Technologies, Sun Yat-sen University, Guangzhou, China

*zhouji@jnu.edu.cn, † qiao@bupt.edu.cn and ‡ lzhh88@sysu.edu.cn

***Abstract*—In recent years, faster-than-Nyquist (FTN) non-orthogonal systems draw more attention for high-capacity communication systems. In this paper, we will introduce digital signal processing for eliminating interference in FTN non-orthogonal systems. FTN non-orthogonal systems can be divided into single-carrier FTN (SC-FTN) and multi-carrier FTN (MC-FTN) non-orthogonal systems. In SC-FTN non-orthogonal systems, joint algorithms will be studied for compensating the serious inter-symbol interference, including joint feed-forward equalizer, post filter and maximum likelihood sequence detection (MLSD) algorithm and joint frequency-domain equalizer and MLSD algorithm. In MC-FTN non-orthogonal systems, inter-carrier interference is similar to the interference in multiple input multiple output (MIMO) systems. The interference cancellation algorithm for MIMO systems is also effective for MC-FTN non-orthogonal systems. We will introduce MIMO decoding to eliminate the interference in MC-FTN non-orthogonal systems.**

***Index Terms*—Digital signal processing, faster than Nyquist, single-carrier non-orthogonal systems, multi-carrier non-orthogonal systems.**

## I. Introduction

In 1970s, Mazo proposed the principle and concept of faster-than-Nyquist (FTN) signaling [1]. FTN signaling can achieve high spectral efficiency, which shows great potential for applications in high-capacity communication systems [2]–[5]. Owing to the resistance of high-frequency distortions, FTN signaling has been widely investigated for optical communications with high baud rate [6]–[9], cost-sensitive short-reach optical communications [10]–[12], and high capacity wireless communications [13]–[15]. The results prove that FTN signaling has a superior performance on the bandwidth-limited communications [16]–[18].

In general, the FTN signaling can be classified into single-carrier and multi-carrier non-orthogonal systems. The single-carrier FTN (SC-FTN) non-orthogonal signal is obtained by compressing the bandwidth of the common single-carrier signal [19]. The multi-carrier FTN (MC-FTN) non-orthogonal signal is generated by further reducing the subcarrier spacing compared to orthogonal frequency-division multiplexing (OFDM) [20]. However, in both SC-FTN and MC-FTN non-orthogonal systems, the bandwidth compression is at the expense of causing the interference. In SC-FTN non-orthogonal system, inter-symbol interference (ISI) caused by the compressed bandwidth degrades the bit error ratio (BER) performance. In MC-FTN non-orthogonal system, the compressed subcarrier spacing induces the inter-carrier interference (ICI), which also degrades the BER performance. Therefore, digital signal processing (DSP) for reducing the serious interferences is key technology in FTN non-orthogonal systems.

In this paper, we will give an overview about DSP for FTN non-orthogonal systems. In SC-FTN non-orthogonal systems, joint algorithms will be studied for compensating the serious ISI, including joint feed-forward equalizer (FFE), post filter and maximum likelihood sequence detection (MLSD) algorithm and joint frequency-domain equalizer (FDE) and MLSD algorithm. In MC-FTN non-orthogonal systems, ICI is similar to the interference in multiple input multiple output (MIMO) systems. The interference cancellation algorithm for MIMO systems is also effective for MC-FTN non-orthogonal systems. We will introduce MIMO decoding to eliminate the interference in MC-FTN non-orthogonal systems.

The rest of this paper is organized as follows. In Section II, DSP for SC-FTN non-orthogonal systems is demonstrated. DSP for MC-FTN Non-Orthogonal Systems is given in Section III. Finally, the paper is concluded in Section IV.

## II. DSP for SC-FTN Non-Orthogonal Systems

In this section, the DSP algorithms are investigated to eliminate the ISI for SC-FTN non-orthogonal systems. In SC-FTN non-orthogonal systems, the bandwidth compression causes the serious ISI, which deteriorates the system performance. For obtaining good system performance, joint algorithm should be used to cancel the serious ISI. The joint FFE, post filter and MLSD algorithm has been widely studied for eliminating the ISI and enhanced in-band noise in SC-FTN non-orthogonal

This work is partly supported by the National Science Foundation of China (NSFC) (U1701661, 61771062); Local Innovation and Research Teams Project of Guangdong Pearl River Talents Program (2017BT01X121); The Youth Science and Technology Innovation Talents of Guangdong (2015TQ01X606); Pearl River S&T Nova Program of Guangzhou (201710010051); The Science and Technology Planning Project of Guangdong Province (2017B010123005). Ji Zhou and Mengqi Guo contributed equally.

©2019 IEEE. Personal use of this material is permitted. Permission from IEEE must be obtained for all other uses, in any current or future media, including reprinting/republishing this material for advertising or promotional purposes, creating new collective works, for resale or redistribution to servers or lists, or reuse of any copyrighted component of this work in other works.

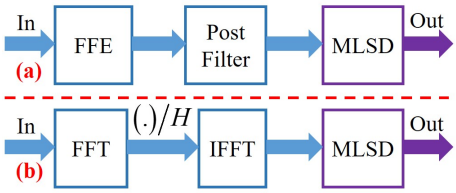


Fig. 1. (a) Structure of joint FFE, post filter and MLSD algorithm; (b) Structure of joint FDE and MLSD algorithm.

systems. Next, the principle of joint FFE, post filter and MLSD algorithm will be introduced.

At the receiver, the received signal can be defined as

$$r(t) = h(t) \otimes x(t) + n(t) \tag{1}$$

where $h(t)$ is channel response. $x(t)$ is transmitted signal. $n(t)$ is adding white Gaussian noise. $\otimes$ denotes convolution operation. Fig. 1 (a) depicts the structure of joint FFE, post filter and MLSD algorithm. First of all, $L$-taps FFE is used to compensate linear distortions. The output of FFE is expressed as

$$x'(t) = \sum_{i=0}^{L-1} a(i) \times r(t - iT) \tag{2}$$

where $a(i)$ is the coefficient of $i$-th tap, which can be calculated by the adaptive algorithms such as least mean square (LMS) and recursive least square (RLS) algorithms. $T$ is the symbol period. If FFE can perfectly compensate the linear distortions, its output is expressed as

$$x'(t) = h^{-1}(t) \otimes r(t) = x(t) + h^{-1}(t) \otimes n(t) \tag{3}$$

where $h^{-1}(t) \otimes n(t)$ depicts that in-band noise is enhanced after FFE. Two-taps post filter is employed to eliminate the enhanced in-band noise. The output of post filter can be expressed as

$$\begin{aligned} z(t) &= h_{\text{PostFilter}}(t) \otimes x(t) + h_{\text{PostFilter}}(t) \otimes h^{-1}(t) \otimes n(t) \\ &= x'(t) + \alpha \times x'(t - T) \end{aligned} \tag{4}$$

where 1 and $\alpha$ are the tap coefficients of post filter. $h_{\text{PostFilter}}(t)$ suppresses the enhanced in-band noise, but causes a known ISI on $x(t)$.

After the FFE and post filter, MLSD is used to cancel the known ISI, which minimizes the Euclidean distance between $z(t)$ and $x(t) + \alpha \times x(t - T)$. The Euclidean distance can be defined as

$$D = \sum_{k} \{z(kT) - [x(kT) + \alpha \times x((kT - T)]\}^2 \tag{5}$$

where $z(kT)$ and $x(kt)$ denote $k$-th sample of $z(t)$ and $x(t)$, respectively. MLSD employs the Viterbi algorithm to obtain the transmitted signal $x(t)$ from the $z(t)$. After joint FFE, post filter and MLSD algorithm, the transmitted signal can be recovered from received SC-FTN signal.

The joint FFE, post filter and MLSD algorithm is a time-domain structure. Due to the serious ISI in SC-FTN signal, FFE needs to use a large number of taps. FFE with large number of taps has high computational complexity, especially when RLS adaptive algorithm is employed. Next, we will introduce an frequency-domain algorithm for SC-FTN non-orthogonal systems.

Figure 1 (b) shows the structure of joint simplified FDE and MLSD algorithm. The frequency-domain version of received signal can be defined as

$$R(f) = H_{\text{channel}}(f) \times X(f) + N(f) \tag{6}$$

In general, FDE can compensate the serious ISI by using frequency-domain channel function $\boldsymbol{H}_{\text{Channel}}$. After ISI compensation, the output of FDE can be expressed as

$$x'(f) = X(f) + N(f)/H_{\text{Channel}}(f) \tag{7}$$

After conventional FDE, the in-band noise is also enhanced. Frequency-domain post filter with transfer function $\boldsymbol{H}_{\text{PostFilter}}$ can be employed to eliminate the enhanced in-band noise. The output of frequency-domain post filter can be expressed as

$$z(f) = H_{\text{PostFilter}} \times X(f) + H_{\text{PostFilter}} \times N(f)/H_{\text{Channel}}(f) \tag{8}$$

Combining the conventional FDE with the frequency-domain post filter, we first design the simplified FDE structure with a transfer function of $\boldsymbol{H} = \boldsymbol{H}_{\text{Channel}}/\boldsymbol{H}_{\text{PostFilter}}$, which can replace the time-domain FFE and post filter structure. Therefore, the output of the simplified FDE structure can be obtained from

$$\boldsymbol{z} = \text{IFFT}(\boldsymbol{R}/\boldsymbol{H}) = \text{IFFT}(\boldsymbol{H}_{\text{PostFilter}} \times \boldsymbol{R}/\boldsymbol{H}_{\text{Channel}}) \tag{9}$$

where $\boldsymbol{R}$ is the frequency-domain received signal, which is equal to FFT($\boldsymbol{r}$). IFFT(.) and FFT(.) denote the inverse fast Fourier transform and fast Fourier transform, respectively. Finally, the MLSD is used to cancel the known ISI after the simplified FDE.

Figure 2 (a) shows the eye diagram of received signal. Due to the noise and channel distortions, the eye diagram of received signal is almost closed. The serious ISI makes the received signal have more than four levels. Fig. 2 (b) depicts the eye diagram of 4-level pulse amplitude modulation (PAM4) signal after FFE or conventional FDE. After FFE or conventional FDE, the ISI can be effectively compensated. However, the in-band noise is enhanced. Therefore, the signal after FFE or conventional FDE has four levels, but is still not clear. Fig. 2 (c) reveals the eye diagram of signal with a known ISI after FFE and post filter or simplified FDE. The post filter eliminates the in-band noise, but causes the known ISI. Therefore, after FFE and post filter or simplified FDE, the signal has clear seven levels.

Figure 3 depicts comparison of BER performance between joint FFE, post filter and MLSD algorithm and joint simplified FDE and MLSD algorithm. The test bench employs 56-Gbit/s optical PAM4 system using 10-G optics over a 10-km standard single-mode fiber (SSMF). In joint FFE, post filter and MLSD algorithm, RLS and LMS adaptive algorithms are employed, respectively. Owing to the lower mean square error (MSE),

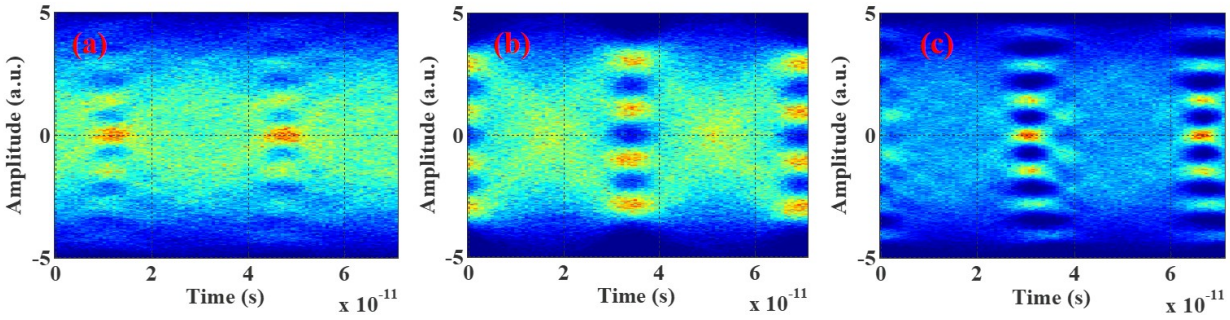


Fig. 2. (a) Eye diagram of received signal; (b) Eye diagram of PAM4 signal after FFE or conventional FDE; (c) Eye diagram of signal with a known ISI after FFE and post filter or simplified FDE.

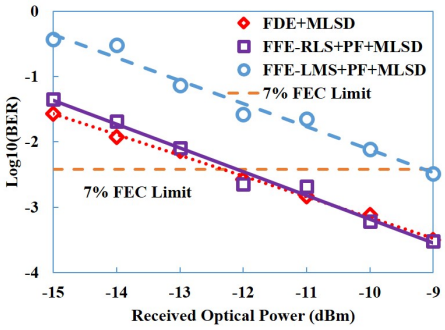


Fig. 3. Comparison of BER performance between joint FFE, post filter and MLSD algorithm and joint simplified FDE and MLSD algorithm.

TABLE I
COMPARISONS AMONG SIMPLIFIED FDE, FFE WITH LMS, AND FFE WITH RLS. $N$ IS THE LENGTH OF FDE. $K$ IS THE TAP NUMBER OF FFE. $M$ IS THE CONSTELLATION SIZE.

| | Computational complexity | Training | Prefix & suffix |
|---|---|---|---|
| FDE | $2\log_2(N)/\log_2(M)$ | Yes | Yes |
| FFE-LMS | $6K/\log_2(M)$ | Yes | No |
| FFE-RLS | $(6K^2+10K)/\log_2(M)$ | Yes | No |

joint FFE with RLS, post filter and MLSD algorithm has better BER performance than joint FFE with LMS, post filter and MLSD algorithm. The joint simplified FDE and MLSD algorithm has the same BER performance compared to the joint FFE with RLS, post filter and MLSD algorithm.

Table I shows the comparisons among the simplified FDE, FFE with LMS, and FFE with RLS. FDE has the lowest computational complexity compared to FFE with LMS and FFE with RLS. However, prefix and suffix should be employed in FDE, which degrades the spectral efficiency. All the schemes requires the training sequence. In conclusion, joint FDE and MLSD algorithm has good performance and low computational complexity at the expense of the addition of prefix and suffix. Joint FFE with RLS, post filter and MLSD algorithm has good performance but ultra-high computational complexity. FFE with LMS is hard to obtain an accepted MSE. Therefore, joint FFE with LMS, post filter and MLSD algorithm requires longer training sequence and cannot achieve the optimal performance.

## III. DSP FOR MC-FTN NON-ORTHOGONAL SYSTEMS

In this section, the DSP techniques are introduced for MC-FTN non-orthogonal systems. The MC-FTN signal is generated by compressing the subcarrier spacing of OFDM, therefore MC-FTN has higher spectral efficiency than OFDM at the expense of ICI. The DSP for MC-FTN non-orthogonal systems mainly focus on ICI cancellation at the receiver.

In MC-FTN non-orthogonal systems with $N$ subcarriers, the received signal $\boldsymbol{Y}$ can be defined as

$$\boldsymbol{Y} = \boldsymbol{C}\boldsymbol{X} + \boldsymbol{W} \tag{10}$$

$\boldsymbol{X}$ is the transmitted signal. $\boldsymbol{C}$ is the correlation matrix represented ICI. $\boldsymbol{W}$ is the white noise. It is revealed from Eq. (10) that the aim of ICI cancellation is to solve a least-square problem, which can be expressed as

$$\tilde{\boldsymbol{X}} = \underset{\boldsymbol{X}\in\mathcal{D}^N}{\arg\min} \|\boldsymbol{Y} - \boldsymbol{C}\boldsymbol{X}\|^2 = \underset{\boldsymbol{X}\in\mathcal{D}^N}{\arg\min} E(\boldsymbol{X}) \tag{11}$$

where $\mathcal{D}$ is the constellation set. $E(\boldsymbol{X})$ is the metric of the signal $\boldsymbol{X}$. Because the MC-FTN non-orthogonal system with $N$ subcarriers can be considered as the MIMO system with $N$ transmitter antennas and $N$ receiver antennas, the interference cancellation algorithms to eliminate interference between antennas are also effective for ICI cancellation in MC-FTN non-orthogonal systems.

Maximum likelihood detection (MLD) is an optimal interference cancellation algorithm in MIMO systems. The optimal solution can be obtained if MLD is used to solve Eq. (11). However, MLD is based on exhaustive search. The exponential increased complexity makes MLD difficult to be used in the practical system. In MIMO decoding, the tree-search algorithms are known as the simplified MLD with near-ML performance. Therefore, tree-search algorithms are more suitable for ICI cancellation than MLD. The commonly used tree-search algorithms can be divided into two categories: depth-first tree search algorithms and breadth-first tree search algorithms. Sphere decoder (SD) is a commonly used decoding algorithm based on depth-first tree search [21]. MLD with QR decomposition and M-algorithm (QRM-MLD) is a commonly

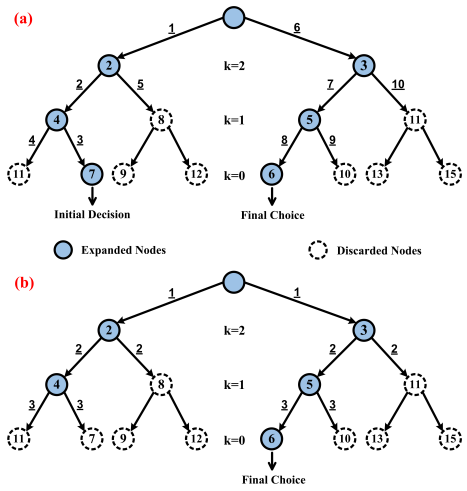


Fig. 4. The examples of search process for (a) SD and (b) QRM-MLD.

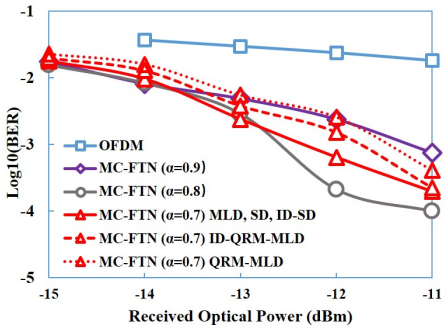


Fig. 5. BER performance of OFDM and MC-FTN with SD, QRM-MLD, ID-SD and ID-QRM-MLD algorithm.

used decoding algorithm based on breadth-first tree search [22]. The details of SD and QRM-MLD are as follows.

Firstly, both the SD and QRM-MLD use QR decomposition (i.e., $\boldsymbol{C} = \boldsymbol{QR}$) to reduce the computational complexity to calculate $E(\boldsymbol{X})$ in Eq. (11). $\boldsymbol{C}$ is decomposed as an $N \times N$ unitary matrix $\boldsymbol{Q}$ and an $N \times N$ upper triangular matrix $\boldsymbol{R}$. Then, $E(\boldsymbol{X})$ can be rewritten as

$$E(\boldsymbol{X}) = \|\boldsymbol{Z} - \boldsymbol{RX}\|^2 = E_{N-1} + E_{N-2} + \cdots + E_0 \quad (12)$$

where $\boldsymbol{Z} = \boldsymbol{Q}^T\boldsymbol{Y}$, and $E_k = \left|Z_k - \sum_{j=k}^{N-1} R_{k,j}X_j\right|^2$ $(0 \leq k \leq N-1)$. Secondly, the final detected symbol $\tilde{\boldsymbol{X}}$ is searched from a tree structure. Fig. 4 shows the examples of search process for SD and QRM-MLD. The numbers beside the branches are the search order. The numbers in the nodes are the accumulated partial metrics $E(\boldsymbol{X}_{k:N-1})$ at the $k$-th subcarrier, that $E(\boldsymbol{X}_{k:N-1}) = E_{N-1} + E_{N-2} + \cdots + E_k$. In SD, the search process performs in both forward and backward directions. The initial search radius is set to infinity. According to Schnorr-Euchner (SE) enumeration, the nodes are visited in the ascending order of their metrics [23]. After an initial decision is obtained, the search radius is reduced to the metric of the initial decision. Then only the path with smaller metric than the search radius is searched. Each time a detected symbol is obtained at the subcarrier 0, the search radius is reduced. In the end, the final detected symbol $\tilde{\boldsymbol{X}}$ with the minimal metric is obtained. In QRM-MLD, the search process performs in forward direction. Only $M_k$ $(0 \leq k \leq N-1)$ paths with the minimal metric are reserved at the $k$-th subcarrer. In the end, the path with the minimal metric is chosen at subcarrier 0, so the final detected symbol $\tilde{\boldsymbol{X}}$ is obtained.

To reduce the computational complexity of SD and QRM-MLD, the initial radius $\beta_I$ calculated by iterative detection (ID) algorithm [24] can be applied before starting the SD and QRM-MLD. The combination of ID algorithm and these two tree-search algorithms respectively are called ID-SD and ID-QRM-MLD in this paper. After adding the initial radius, both ID-SD and ID-QRM-MLD only search the candidate solutions within $\beta_I$. If the solution is not found within $\beta_I$, the initial solution $\boldsymbol{S}_I$ calculated by ID algorithm is chosen as the final detected symbol.

To show the transmission performance of MC-FTN signal with ICI cancellation algorithms, 28-Gbit/s MC-FTN non-orthogonal system is experimentally demonstrated with 10-G optics over a 10-km SSMF. The 3-dB equivalent bandwidth of this system is approximately 5.5 GHz. The modulation signal on each subcarrier is PAM2. As shown in Fig. 5, the BER performance of MC-FTN is much better than that of OFDM, because OFDM suffers serious high-frequency distortion caused by bandwidth limitation. In MC-FTN, the bandwidth compression factors $\alpha$ is set to 0.9, 0.8 and 0.7. MC-FTN with $\alpha = 0.8$ has better performance than MC-FTN with $\alpha = 0.9$ or $\alpha = 0.7$, because MC-FTN with $\alpha = 0.9$ suffers more influence from high-frequency distortion and MC-FTN with $\alpha = 0.7$ suffers more influence from ICI.

When comes to the ICI cancellation performances of SD, QRM-MLD, ID-SD and ID-QRM-MLD, it is revealed from Fig. 5 that all of SD, QRM-MLD, ID-SD and ID-QRM-MLD can achieve the same ICI cancellation performance as MLD in MC-FTN with $\alpha = 0.9$ and $\alpha = 0.8$. The ICI cancellation performance of MLD is served as a benchmark. The ICI is increased in MC-FTN with $\alpha = 0.7$, under this condition SD and ID-SD still can achieve the same ICI cancellation performance as MLD, but QRM-MLD and ID-QRM-MLD have worse performance due to the limited $M_k$ value. For ID-QRM-MLD, when the metrics of all the reserved paths are larger than the initial radius, the search process is stopped and $\boldsymbol{S}_I$ is chosen as the final detected symbol, therefore ID-QRM-MLD has better performance than QRM-MLD.

Figure 6 depicts the computational complexity of SD, QRM-MLD, ID-SD and ID-QRM-MLD represented by the number of expanded nodes [25]. Because the running time of the tree-search algorithm is much longer than the running time of ID algorithm, the number of expanded nodes can be used to represent the computational complexity of these algorithms. The computational complexity of SD is changed according to ICI. The computational complexity of QRM-MLD is related to the fixed $M_k$ value. ID-SD and ID-QRM-MLD have lower

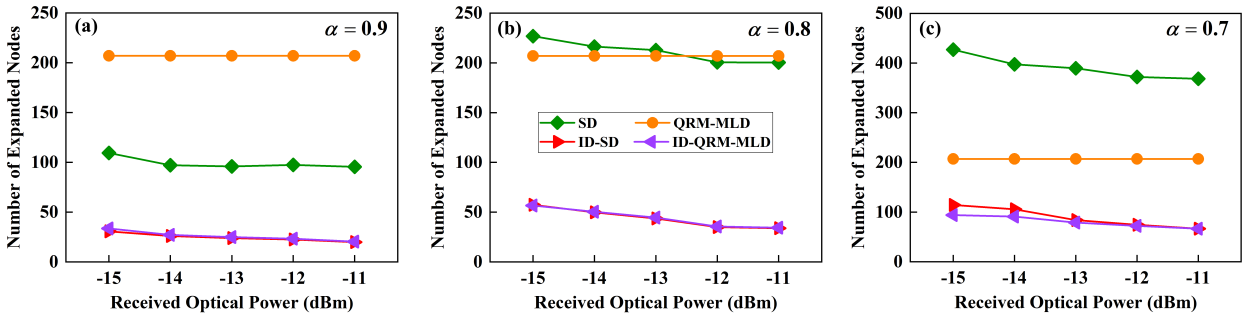


Fig. 6. The computational complexity represented by the number of expanded nodes for SD, QRM-MLD, ID-SD and ID-QRM-MLD in MC-FTN with $\alpha = 0.9,\ 0.8 and\ 0.7$ [25].

computational complexity than SD and QRM-MLD. In conclusion, if the best BER performance of MC-FTN non-orthogonal systems is needed to obtain directly, ID-SD is preferred. If the BER performance and computational complexity of MC-FTN non-orthogonal systems are needed to be flexibly adjusted through changing $M_k$ value, ID-QRM-MLD is preferred.

## IV. Conclusions

In this paper, we introduce DSP algorithms for FTN non-orthogonal systems in detail. In SC-FTN non-orthogonal systems, three joint algorithms are investigated for compensating the serious ISI, including their performance, efficiency, and computational complexity. In MC-FTN non-orthogonal systems, the interference cancellation algorithms in MIMO systems are effective for MC-FTN non-orthogonal systems. We have investigated the popular MIMO decoding algorithms for eliminating the ICI in MC-FTN non-orthogonal systems. In conclusion, this paper gives an overview of DSP for FTN non-orthogonal systems, which can offer some references for the researches in next generation high-capacity communications.

## References


[1] J. E. Mazo, "Faster-Than-Nyquist Signaling," *The Bell System Technical Journal*, vol. 54, no. 8, pp.1451–1462, Oct. 1975.

[2] J. B. Anderson, F. Rusek, and O. Viktor, "Faster-Than-Nyquist Signaling," *Proceedings of the IEEE*, vol. 101, no. 8, pp. 1817–1830, Aug. 2013.

[3] J. Fan et al., "Faster-Than-Nyquist Signaling: An Overview," *IEEE Access*, vol. 5, pp. 1925–1940, Feb. 2017.

[4] J. Yu et al., "Transmission of 8×480-Gb/s super-Nyquist-filtering 9-QAM-like signal at 100 GHz-grid over 5000-km SMF-28 and twenty-five 100 GHz-grid ROADMs," *Optics Express*, vol. 21, no. 13, pp. 15686–15691, July. 2013.

[5] J. Man et al., "Downstream Transmission of Pre-Distorted 25-Gb/s Faster-than-Nyquist PON with 10G-Class Optics Achieving over 31 dB Link Budget without Optical Amplification," in *Optical Fiber Communication Conference*, March 2016, paper Th1I.5.

[6] C. Prodaniuc et al., "Partial response signaling for improved chromatic dispersion tolerance in intensity modulation optical transmissions," *Optics Express*, vol. 26, no. 3, pp. 3013–3019, Feb. 2018.

[7] Q. Zhang et al., "Up to 190-Gb/s OOK Signal Generation using a Coding and Cutting Technique with a 92 GSa/s DAC," in *Optical Fiber Communication Conference*, March 2017, paper Th3D.1.

[8] J. Zhang, J. Yu, and N. Chi, "Generation and transmission of 512-Gb/s quad-carrier digital super-Nyquist spectral shaped signal," *Optics Express*, vol. 21, no. 25, pp. 31212–31217 , Dec. 2013.

[9] D. Semrau et al., "Achievable information rates estimates in optically amplified transmission systems using nonlinearity compensation and probabilistic shaping," *Optics Letters*, vol. 42, no. 1, pp. 121–124, 2017.

[10] J. Man et al., "25-Gb/s and 40-Gb/s Faster-than-Nyquist PON Based on Low-Cost 10G-Class Optics," in *Asia Communications and Photonics Conference*, Nov. 2015, paper AM1F.1.

[11] J. Zhou et al., "Faster-than-Nyquist non-orthogonal frequency-division multiplexing based on fractional Hartley transform," *Optics Letters*, vol. 41, no. 19, pp. 4488–4491, Oct. 2016.

[12] K. Zhong et al., "Digital Signal Processing for Short-Reach Optical Communications: A Review of Current Technologies and Future Trends," *Journal of Lightwave Technology*, vol. 36, no. 2, pp. 377-400, Jan. 2018.

[13] M. E. Hefnawy and H. Taoka, "Overview of Faster-Than-Nyquist for Future Mobile Communication Systems," in *Vehicular Technology Conference*, June 2013, pp. 1–5.

[14] T. Xu and I. Darwazeh,"Transmission experiment of bandwidth compressed carrier aggregation in a realistic fading channel," *IEEE Transactions on Vehicular Technology*, vol. 66, no. 5, pp. 4087–4097, May 2017.

[15] T. Xu and I. Darwazeh,"Non-Orthogonal Narrowband Internet of Things: A Design for Saving Bandwidth and Doubling the Number of Connected Devices," *IEEE Internet of Things Journal*, vol. 5, no. 3, pp. 2120–2129, April 2018.

[16] N. Chi, J. Zhao, and Z. Wang,"Bandwidth-efficient visible light communication system based on faster-than-Nyquist pre-coded CAP modulation,"*Chinese Optics Letters*, vol. 15, p. 080601, Aug. 2017.

[17] J. Zhou et al.,"Faster-Than-Nyquist Non-Orthogonal Frequency-Division Multiplexing for Visible Light Communications,"*IEEE Access*, vol. 6, pp. 17933–17941, March 2018.

[18] J. Zhou et al., "Capacity limit for faster-than-Nyquist non-orthogonal frequency-division multiplexing signaling," *Scientific Reports*, vol. 7, May 2017, Article No. 3380.

[19] J. Li, E. Tipsuwannakul, T. Eriksson, M. Karlsson and P. A. Andrekson, "Approaching Nyquist Limit in WDM Systems by Low-Complexity Receiver-Side Duobinary Shaping," *Journal of Lightwave Technology*, vol. 30, no. 11, pp. 1664–1676, 2012.

[20] I. Kanaras, A. Chorti, M. R. D. Rodrigues, and I. Darwazeh,"Spectrally efficient FDM signals: Bandwidth gain at the expense of receiver complexity," in *IEEE International Conference on Communications*, June 2009, pp.1–6.

[21] B. Hassibi and H. Vikalo, "On the sphere-decoding algorithm I. expected complexity," *IEEE Trans. Signal Process.*, vol. 53, no. 8, pp. 2806–2818, Aug. 2005.

[22] M. Guo et al., "Simplified Maximum Likelihood Detection for FTN Non-Orthogonal FDM System," *IEEE Photonics Technology Letters*, vol. 29, no. 19, pp. 1687–4491, Oct. 2017.

[23] C. P. Schnorr and M. Euchner, "Lattice basis reduction: Improved practical algorithms and solving subset sum problems," *Math. Programming*, vol. 66, pp. 181–191, 1994.

[24] T. Xu, R. C. Grammenos, F. Marvasti, and I. Darwazeh, "An improved fixed sphere decoder employing soft decision for the detection of non-orthogonal signals," *IEEE Communications Letters*, vol. 17, no. 10, pp. 1964–1967, 2013.

[25] M. Guo, Y. Qiao, J. Zhou, X. Tang, J. Qi, S. Liu, X. Xu and Y. Lu, "ICI Cancellation Based on MIMO Decoding for FTN Non-Orthogonal FDM Systems," *Journal of Lightwave Technology*, vol. 37, no. 3, pp. 1045–1055, 2019.